IFAC

IFAC
INTERNATIONAL FEDERATION
of AUTOMATIC CONTROL

Preprints

ALGORITHMS and ARCHITECTURES for REAL-TIME CONTROL

Edited by A. E. RUANO

AARTC '97

Vilamoura, Portugal, 9-11 April 1997

APCA
PORTUGUESE SOCIETY of
AUTOMATIC CONTROL

Preprints of the 4th IFAC Workshop on
Algorithms and Architectures for Real-Time Control

VARIABLE STRUCTURE POSITION/FORCE HYBRID CONTROL OF MANIPULATORS

J. A. Tenreiro Machado and Abílio Azenha

Department of Electrical and Computer Engineering, Faculty of Engineering,
University of Porto
Rua dos Bragas, 4099 Porto Codex, Portugal
Phone: +351-2-317105, Fax: +351-2-319280/2003610,
E-mail: jtm@fe.up.pt, azenha@tom.fe.up.pt

Abstract: In this paper it is studied the implementation of a variable structure algorithm in the position/force hybrid control of robotic manipulators. The frequency response of the system is calculated and it is found to have good performances. An introduction to describing function analysis of the system is also included and effect of the controller sampling frequency is analysed.

Keywords: Robotics, Manufacturing Systems, Intelligent Control, Variable Structure Systems, Force Control.

1. INTRODUCTION

As the demand for high quality and low cost products increases, the need for process automation grows rapidly. Therefore, the introduction of robotic systems in the manufacturing of goods is a major interest in the production system. In this perspective, this paper presents a study on position/force control of robot manipulators required in automated processes that involve contact between the end--effector of the arm and the environment. Such tasks are, for example, deburring, assembly, grinding and spot welding, because they need control of both the position and the force of the robot tool.

In the early eighties Raibert and Craig (1981) introduced the concept of force control based on the hybrid algorithm. Since then, several researchers (Mason, 1981; Khatib, 1987; Whitney, 1987; Hogan, 1985; Zhang and Paul, 1985) developed these ideas and proposed new algorithms such as the impedance controller. Problems with position/force control are further investigated in An and Hollerbach (1987) and Fisher and Mujtaba (1992), while more advanced, and recent, studies of this algorithm can be found in Siciliano and Villani (1996) and Volpe and Khosla (1994). Nevertheless, this area of research is only beginning to emerge from the *sea* of unexplored problems of sustained contact between the robot and the workpiece. In this line of thought, this paper presents a robust algorithm for this type of robot control that only needs a force sensor in the wrist of the arm in addition to velocity and position measurements of the joint coordinates.

The article is organised as follows. Section two introduces the position/force control algorithm. Section three shows some results with variable structure controllers (VSCs) in the position and force control loops. Section four presents the frequency response of the closed-loop system, while section five studies the stability of the system through a linearization. Finally, section six outlines the main conclusions.

2. THE POSITION/FORCE HYBRID CONTROLLER

The dynamic equation of an ideal rigid-link-rigid--joint robot with n links interacting with the environment is:

$$\boldsymbol{\tau} = \mathbf{H}(\mathbf{q})\ddot{\mathbf{q}} + \mathbf{c}(\mathbf{q},\dot{\mathbf{q}}) + \mathbf{g}(\mathbf{q}) - \mathbf{J}^T(\mathbf{q})\mathbf{F} \qquad (1)$$

Here $\boldsymbol{\tau}$ is the $n \times 1$ vector of actuator torques. $\mathbf{q}$ is the $n \times 1$ vector of joint coordinates, $\mathbf{H}(\mathbf{q})$ is the $n \times n$ inertia matrix, $\mathbf{c}(\mathbf{q},\dot{\mathbf{q}})$ is a $n \times 1$ vector of centrifugal/Coriolis terms and $\mathbf{g}(\mathbf{q})$ is the $n \times 1$ vector of gravitational effects. The $n \times n$ matrix $\mathbf{J}^T(\mathbf{q})$ is the transpose of the Jacobian matrix of the robot and $\mathbf{F}$ is the $n \times 1$ vector of the force that the environment exerts in the robot end-effector.

In this study we shall adopt as prototype manipulator the 2R robot with dynamics given by:

$$\mathbf{H}(\mathbf{q}) = \begin{bmatrix} (m_1+m_2)r_1^2 + m_2 r_2^2 + & m_2 r_2^2 + m_2 r_1 r_2 C_2 \\ +2m_2 r_1 r_2 C_2 + J_{1m} + J_{1g} & \\ m_2 r_2^2 + m_2 r_1 r_2 C_2 & m_2 r_2^2 + J_{2m} + J_{2g} \end{bmatrix}$$

$$\mathbf{c}(\mathbf{q},\dot{\mathbf{q}}) = \begin{bmatrix} -m_2 r_1 r_2 S_2 \dot{q}_2^2 - 2m_2 r_1 r_2 S_2 \dot{q}_1 \dot{q}_2 \\ m_2 r_1 r_2 S_2 \dot{q}_1^2 \end{bmatrix} \qquad (2)$$

$$\mathbf{g}(\mathbf{q}) = \begin{bmatrix} g(m_1 r_1 C_1 + m_2 r_1 C_1 + m_2 r_2 C_{12}) \\ g m_2 r_2 C_{12} \end{bmatrix}$$

$$\mathbf{J}^T(\mathbf{q}) = \begin{bmatrix} -r_1 S_1 - r_2 S_{12} & r_1 C_1 + r_2 C_{12} \\ -r_2 S_{12} & r_2 C_{12} \end{bmatrix}$$

where $C_i = \cos(q_i)$, $C_{ij} = \cos(q_i + q_j)$, $S_i = \sin(q_i)$, $S_{ij} = \sin(q_i + q_j)$ and a constraint plane determined by the angle θ as depicted in Fig. 1. The numerical values adopted for the ideal 2R robot are enumerated in Table 1.

Table 1 The 2R robot parameters.

i	m_i (Kg)	r_i (m)	J_{im} (Kgm^2)	J_{ig} (Kgm^2)
1	0.5	1.0	1.0	4.0
2	6.25	0.8	1.0	4.0

As usual, the contact of the robot with the constraint surface is modelled through a linear system with a mass M, a damping coefficient B and a stiffness K. The adoption of the alternative model of a dashpot with two springs (Azenha and Machado, 1997) was also investigated leading to the same kind of conclusions. The schematic structure of the position/force hybrid control algorithm is depicted in Fig. 2. The matrix $\mathbf{I}$ is the $n \times n$ identity matrix and the diagonal matrix $\mathbf{S}$ is the $n \times n$ selection matrix with elements equal to one in the position controlled directions and zero in the force controlled directions. In this paper we consider the x_C Cartesian coordinate to be force controlled and y_C Cartesian coordinate to be position controlled (3).

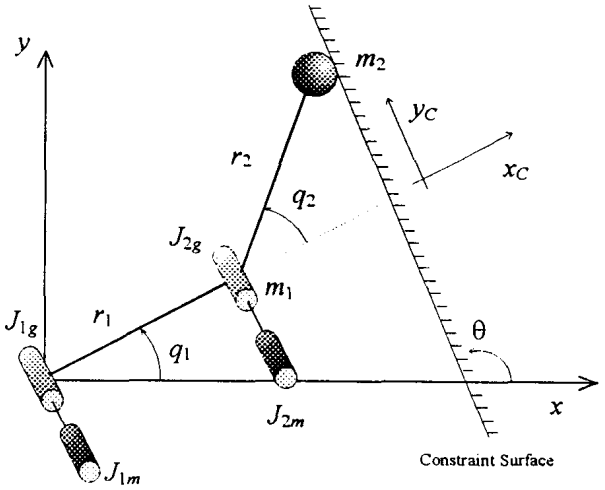

Fig. 1 The ideal 2R robot and the constraint surface.

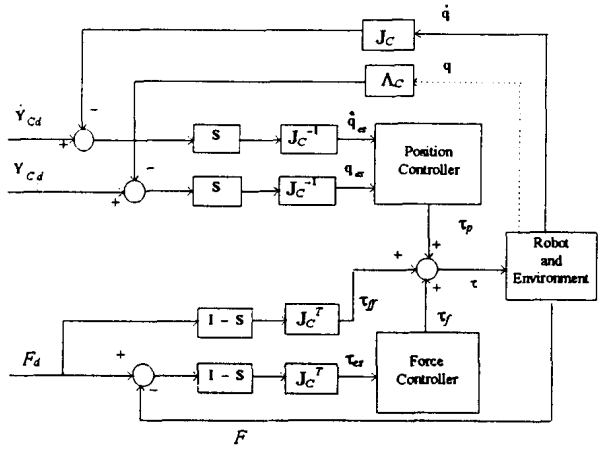

Fig. 2 Block diagram of the position/force hybrid control algorithm.

$$\mathbf{S} = \begin{bmatrix} 0 & 0 \\ 0 & 1 \end{bmatrix} \qquad (3)$$

$$\mathbf{J}_C(\mathbf{q}) = \begin{bmatrix} -r_1 C_{\theta 1} - r_2 C_{\theta 12} & -r_2 C_{\theta 12} \\ r_1 S_{\theta 1} + r_2 S_{\theta 12} & r_2 S_{\theta 12} \end{bmatrix}$$

$$\Lambda_C: \begin{cases} x_C = r_1 S_{\theta 1} + r_2 S_{\theta 12} \\ y_C = r_1 C_{\theta 1} + r_2 C_{\theta 12} \end{cases}$$

where $C_{\theta 1} = \cos(\theta - q_1)$, $C_{\theta 12} = \cos(\theta - q_1 - q_2)$, $S_{\theta 1} = \sin(\theta - q_1)$ and $S_{\theta 12} = \sin(\theta - q_1 - q_2)$.

3. SOME SIMULATION RESULTS

In this section we study the system response using VSCs, both at the position and force control loops (with a sampling frequency of f_c = 10 kHz), instead of the standard PID algorithms. The constraint surface parameters are M = 0 Kg, B = 1 Ns/m and K = 100 N/m.

In a first case study, the position controller is the first-order VSC (Azenha and Machado, 1996; Machado and de Carvalho, 1988; Utkin, 1977; Young, 1978) with sliding surface ($c_{Pi} = 2.5\ s^{-1}$, i = 1,2) and control effort given by the equations (4).

$$\mathbf{q}_{es} = \mathbf{J}_C^{-1}\mathbf{S}\left(\mathbf{Y}_{cd} - \mathbf{Y}_c\right) \quad (4a)$$

$$\sigma_i = \dot{q}_{esi} + c_{Pi} q_{esi} \quad (4b)$$

$$\tau_{VSCi} = \begin{cases} \tau_{Pmaxi} & ,\sigma_i \geq \tau_{Pmaxi} / K_{Pi} \\ K_{Pi}\sigma_i & ,|\sigma_i| < \tau_{Pmaxi} / K_{Pi} \\ -\tau_{Pmaxi} & ,\sigma_i \leq -\tau_{Pmaxi} / K_{Pi} \end{cases} \quad (4c)$$

The force controller is the VSC ($c_{Fi} = 0.25\ s^{-1}$, $i = 1,2$):

$$\tau_{es} = \mathbf{J}_C^T\left(\mathbf{I} - \mathbf{S}\right)\left(\mathbf{F}_d - \mathbf{F}\right) \quad (5a)$$

$$\sigma_i = \tau_{esi} + c_{Fi}\int \tau_{esi} dt \quad (5b)$$

$$\tau_{VSCi} = \begin{cases} \tau_{Fmaxi} & ,\sigma_i \geq \tau_{Fmaxi} / K_{Fi} \\ K_{Fi}\sigma_i & ,|\sigma_i| < \tau_{Fmaxi} / K_{Fi} \\ -\tau_{Fmaxi} & ,\sigma_i \leq -\tau_{Fmaxi} / K_{Fi} \end{cases} \quad (5c)$$

Table 2 shows the numerical values of the control effort block adopted in this section.

Table 2 Numerical values of the VSCs.

Joint i	K_{Pi}	K_{Fi}	τ_{Pmaxi}	τ_{Fmaxi}
1	10,000	100	1,000	1,000
2	10,000	100	500	500

In Fig. 3 we present the time response for a position step input of 0.1 m (δy_C) established at $t = 3$ (to damp out the initial conditions), $\theta = \pi/2$ and the initial operating point $q_{10} = q_{20} = \pi/2$, where q_{i0} stands for $q_i(t = 0)$, $i = 1,2$.

In Fig. 4 an alternative experiment, shows the time response for a force step input of 1 N (δF_d) at $t = 3$, $\theta = \pi/2$ and the same initial operating point $q_{10} = q_{20} = \pi/2$.

In a second case study we introduce an integral term in the sliding surface of the position-VSC as described in equations (6). The parameters of the sliding surface are $\omega_{ni} = 7.91\ rads^{-1}$ and $\xi_i = 1.74$ ($i = 1,2$). By this way, the dominant eigenvalue of the sliding surface remains unchanged. This controller enables us to have small position errors, because of the integral action in the second order sliding surface. In this line of thought, Figs. 5 and 6 present the system time responses for the same two test input signals.

$$\mathbf{q}_{es} = \mathbf{J}_C^{-1}\mathbf{S}\left(\mathbf{Y}_{cd} - \mathbf{Y}_c\right) \quad (6a)$$

$$\sigma_i = \dot{q}_{esi} + 2\omega_{ni}\xi_i q_{esi} + \omega_{ni}^2 \int q_{esi} dt \quad (6b)$$

$$\tau_{VSCi} = \begin{cases} \tau_{Pmaxi} & ,\sigma_i \geq \tau_{Pmaxi} / K_{Pi} \\ K_{Pi}\sigma_i & ,|\sigma_i| < \tau_{Pmaxi} / K_{Pi} \\ -\tau_{Pmaxi} & ,\sigma_i \leq -\tau_{Pmaxi} / K_{Pi} \end{cases} \quad (6c)$$

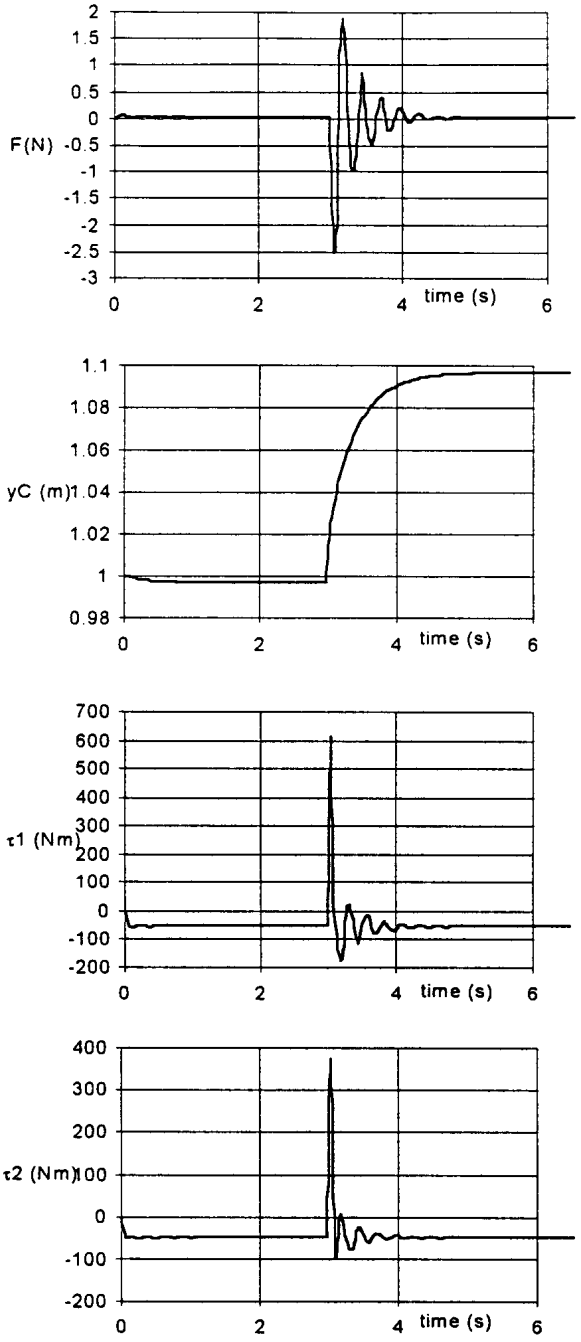

Fig. 3 Time responses of the position/force hybrid control system for a step position (δy_{Cd}) input: Force; Position; Torque at joint 1; Torque at joint 2.

As can be seen in Figs. 3-4 and Figs. 5-6, the second-order VSC in the position control loop leads to much smaller steady-state position errors, while the transient remains approximately the same.

4. FREQUENCY RESPONSE OF THE SYSTEM

In this section we start by choosing a second system operating point, because it is important to study the controller performance under different conditions. In this line of thought, the initial parameters are $\theta = \pi/2$, $q_{10} = q_{20} = 15\pi/36$, $K = 100$ N/m, $B = 1$ Ns/m and $M = 0$ Kg (case study 3).

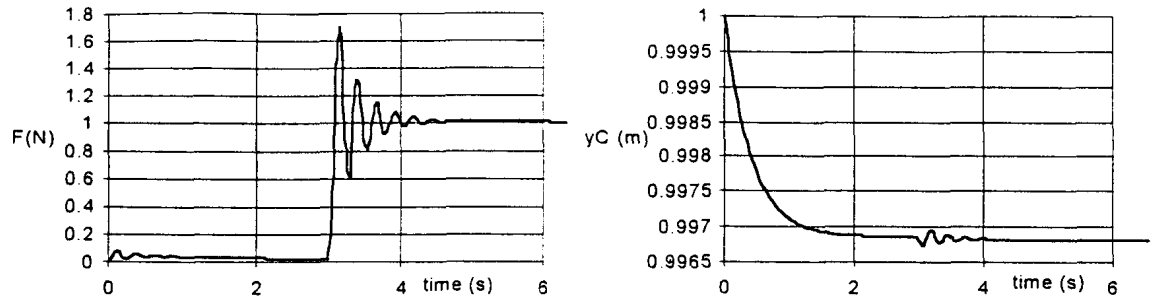

Fig. 4 Time responses of the position/force hybrid control system for a step force (δF_d) input: Force; Position.

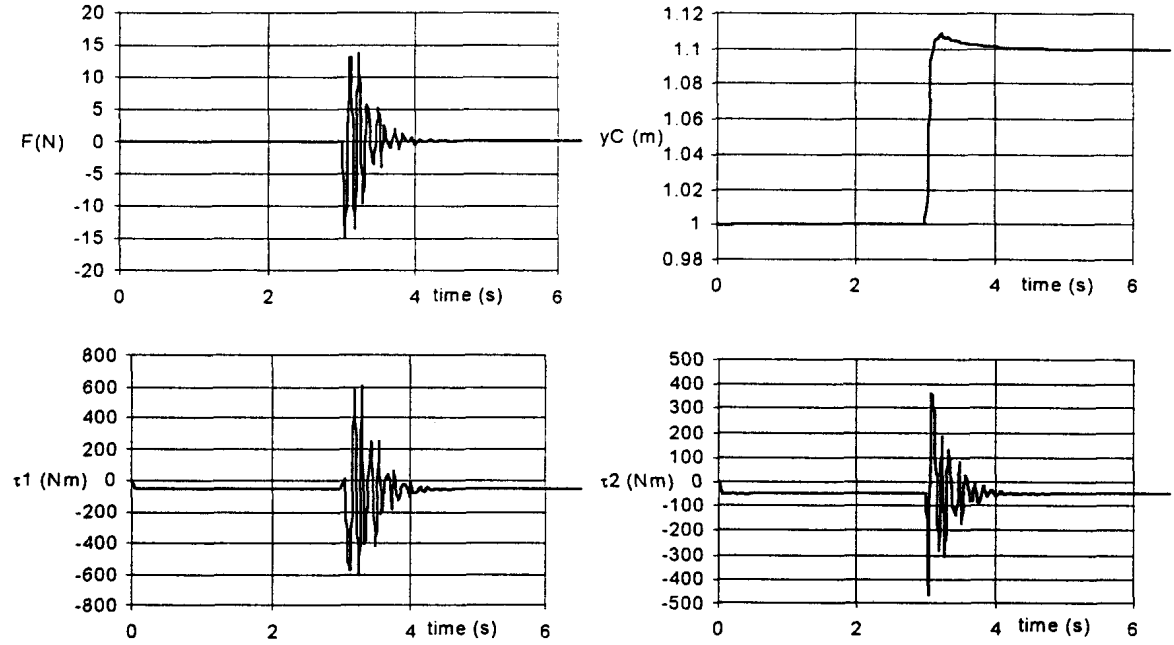

Fig. 5 Time responses of the position/force hybrid control system for a step position (δy_{Cd}) input: Force; Position; Torque at joint 1; Torque at joint 2.

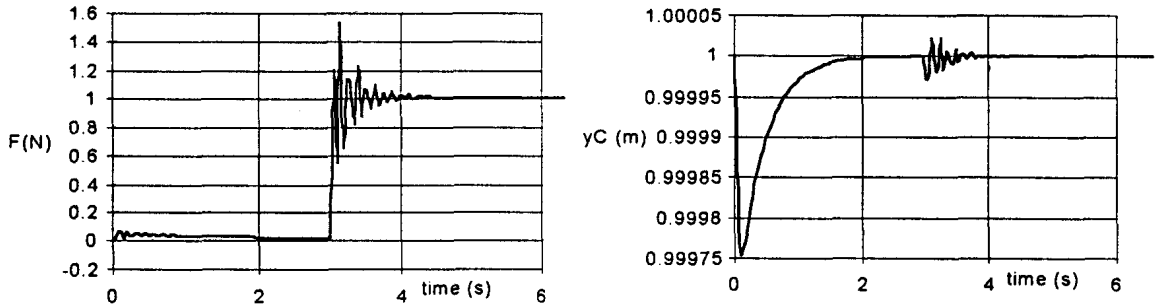

Fig. 6 Time responses of the position/force hybrid control system for a step force (δF_d) input: Force; Position.

Fig. 7 shows the frequency response (f.r.) of the system for the position first order VSC presented previously, and two different amplitude input signals $\delta y_{Cd} = 0.03$ m or $\delta y_{Cd} = 0.1$ m and $\delta F_d = 1$ N or $\delta F_d = 4$ N. The f.r. of the system for the case study 1 is nearly the same and, therefore, it is not presented. On the other hand, for the f.r. of case study 2 (Fig. 8) we get a slightly different f.r. Nevertheless, the overall characteristics remain almost unchanged revealing that the VSC-hybrid controller is robust against operating point variations. Moreover, from Figs. 7-8 we conclude that the f.r. has low sensitivity to the amplitude of the reference signal, meaning that the system has a behaviour such as a linear one. The low-pass responses of $|Y_C/Y_{Cd}|$ and $|F/F_d|$ have a cut-off frequency that depends on the environment parameters. In particular, the resonance peak f_0 of $|F/F_d|$ is very sensitive while $|Y_C/Y_{Cd}|$ has a much smaller sensitivity. In $|Y_C/F_d|$ and $|F/Y_{Cd}|$ we have bandpass f.r.s with resonance peaks also at f_0.

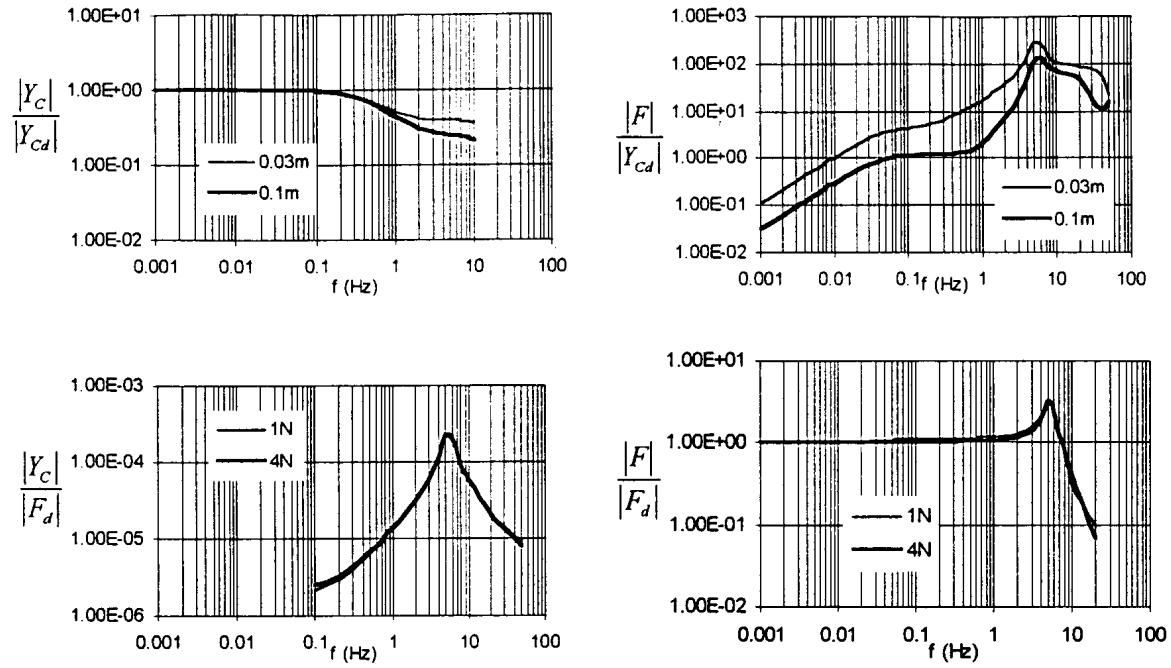

Fig. 7 Frequency responses of the position/force hybrid VSC (case study 3, $q_{10} = q_{20} = 15\pi/36$).

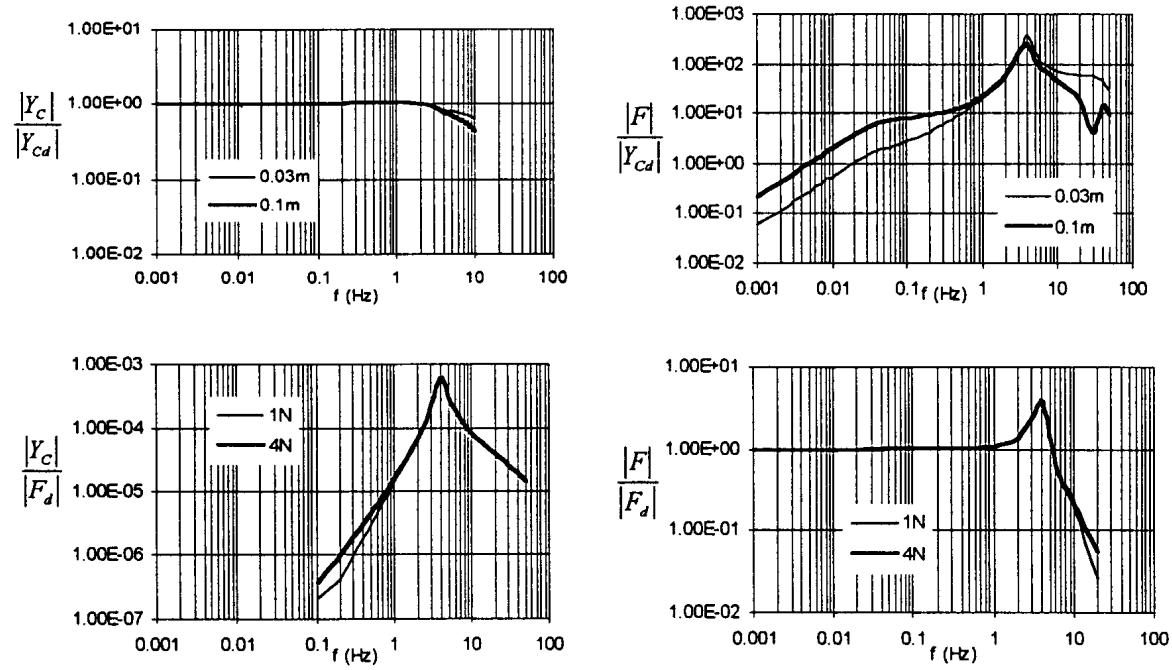

Fig. 8 Frequency responses of the position/force hybrid VSC (case study 2, $q_{10} = q_{20} = \pi/2$).

Another important system characteristic to study is the effect of the controller sampling frequency upon the system performances. The experiments showed that f_c = 10 kHz is a controller frequency that leads to good results. Nevertheless, for operating points with an high damping coefficient B it is found that frequencies down to f_c = 500 Hz are acceptable being the f.r.s nearly the same.

5. STABILITY ANALYSIS THROUGH LINEARIZATION

In this section it is presented an analysis of the system stability through its linearization.

Notice that, for analysing the system stability with large amplitude signals, we must employ, in general, the describing function (Atherton, 1975) instead of the linearization. Nevertheless, the observed limit cycles revealed small amplitudes and, therefore, the linearization method is sufficient.

The system equations can be simplified resulting the MIMO system equations:

$$\begin{cases} Q_1 = N_{11}Q_1 + N_{21}Q_2 \\ Q_2 = N_{12}Q_1 + N_{22}Q_2 \end{cases} \tag{7}$$

where Q_i stands for the Laplace transform of q_i

(i = 1,2). Then we can apply Nyquist multivariable criterion which leads to the characteristic equation:

$$N_{11}N_{22} - N_{11} - N_{22} - N_{12}N_{21} + 1 = 0 \quad (8)$$

We found a limit cycle with an oscillation of 5 Hz for $\theta = \pi/2$, $q_{10} = q_{20} = 15\pi/36$, $K = 100$ N/m, $B = 0.03$ Ns/m and $M = 0$ Kg. The frequency of the limit cycle is the same, both in the analytical and experimental results.

The Nyquist diagram of the system for several controller frequencies is shown in Fig. 9. The results agree with the simulation. In fact, for $f_c = 10$ kHz the limit cycle is stable while decreasing f_c the system becomes unstable.

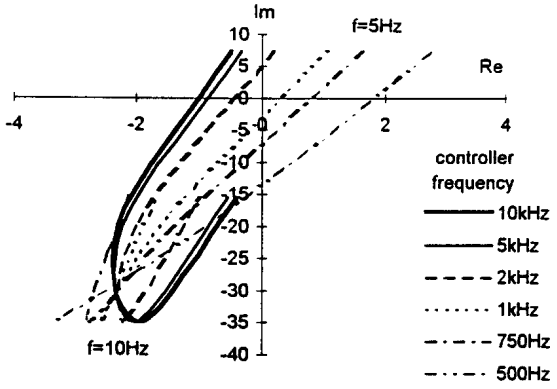

Fig. 9 Nyquist diagram of the system for several controller frequencies.

6. CONCLUSIONS

This paper presented the design and implementation of position/force hybrid VSC of robot manipulators. Several controllers and operating conditions were studied and the second order VSC was shown to be superior, because it reduced the steady-state position error. Frequency response techniques were also employed in the characterisation of system behaviour and good linearity properties were found. The stability and accuracy of the system are shown to be satisfactory and some practical and real time considerations are made, by studying the influence of sampling frequency.

ACKNOWLEDGEMENT

This paper was developed under the grant PRAXIS XXI/BD/4524/94 from JNICT.

REFERENCES

An, C. H. and J. M. Hollerbach (1987). Kinematic Stability Issues in Force Control of Manipulators, *Proc. of the IEEE Int. Conf. on Robotics and Automation*, pp. 897-903.

Atherton, D. P. (1975). *Nonlinear Control Engineering*, Van Nostrand Reinhold Company, London.

Azenha, A. and J. A. T. Machado (1996). Variable Structure Control of Systems with Nonlinear Friction and Dynamic Backlash, *IFAC 13th World Congress*, San Francisco, California, USA, vol. E, pp. 515-520.

Azenha, A. and J. A. T. Machado (1997). On the Variable Structure Position/Force Hybrid Control of Manipulators, *submitted to the 1997 IEEE International Symposium on Computational Intelligence in Robotics and Automation*, Monterey, California, USA.

Fisher, W. D. and M. S. Mujtaba (1992). Sufficient Stability Condition for Hybrid Position/Force Control, *Proc. of the Int. Conf. on Robotics and Automation*, Nice, France, pp. 1336-1341.

Hogan, N. (1985). Impedance Control: An Approach to Manipulation, Parts I-Theory, II-Implementation and III-Applications, *ASME Journal of Dynamic Systems, Measurement, and Control*, **107**, No. 1, pp. 1-24.

Khatib, O. (1987). A Unified Approach for Motion and Force Control of Robot Manipulators: The Operational Space Formulation, *IEEE Journal of Robotics and Automation*, **3**, No. 1, pp. 43-53.

Machado, J. A. T. and J. L. M. de Carvalho (1988). A New Variable Structure Controller for Robot Manipulators, *IEEE International Symposium on Intelligent Control*, USA.

Mason, M. T. (1981). Compliance and Force Control for Computer Controlled Manipulators, *IEEE Transactions on Systems, Man, and Cybernetics*, **11**, No. 1, pp. 418-432.

Raibert, M. H. and J. J. Craig (1981). Hybrid Position/Force Control of Manipulators, *ASME Journal of Dynamic Systems, Measurement, and Control*, **102**, No. 2, pp. 126-133.

Siciliano, B. and L. Villani (1996). A Force/Position Regulator for Robot Manipulators Without Velocity Measurements, *IEEE International Conference on Robotics and Automation*, Minneapolis, USA, pp. 2567-2572.

Utkin, V. I. (1977). Variable Structure Systems With Sliding Modes, *IEEE Transactions on Automatic Control*, **22**, pp. 212-222.

Volpe, R. and P. Khosla (1994). Computational Considerations in the Implementation of Force Control Strategies, *Journal of Intelligent and Robotic Systems*, **9**, pp. 121-148.

Whitney, D. E. (1987). Historical Perspective and State of the Art in Robot Force Control, *The Int. J. of Robotics Research*, **6**, No. 1, pp. 3-14.

Young, K.-K. D. (1978). Controller Design for a Manipulator Using Theory of Variable Structure Systems, *IEEE Transactions on Systems, Man, and Cybernetics*, **8**, No. 2, pp. 101-109.

Zhang, H. and R. P. Paul (1985). Hybrid Control of Robot Manipulators, *Proc. of the IEEE Int. Conf. on Robotics and Automation*, USA, pp. 602-607.